Available online at www.sciencedirect.com
SCIENCE DIRECT®
Measurement 37 (2005) 63–76
Measurement
www.elsevier.com/locate/measurement

An application of the independent component analysis to monitor acoustic emission signals generated by termite activity in wood

J.J. Gonzalez de la Rosa [a,*], C.G. Puntonet [b], I. Lloret [c]

[a] Research Group in Applied Electronics Instrumentation, Engineering School of Algeciras, University of Cádiz, Av. Ramón, Puyol S/N. 11202 Algeciras-Cádiz, Spain
[b] Department of Architecture and Computers Technology, University of Granada, ESII, C/Periodista Daniel Saucedo, 18071 Granada, Spain
[c] Department of Computer Science, Engineering School of Algeciras, University of Cádiz, Av. Ramón Puyol S/N, 11202 Algeciras-Cádiz, Spain

Received 13 January 2004; accepted 26 August 2004
Available online 7 October 2004

Abstract

In this paper an extended robust independent components analysis (ERICA) algorithm based on cumulants is applied to identify vibrational alarm signals generated by soldier termites in southern Spain (reticulitermes grassei), by drumming their heads against the substratum, and measured by low cost equipment. A seismic accelerometer is employed to strongly characterize these acoustic emissions. To support the proposed technique, vibrational signals from a low cost microphone have been mixed with known signals, and the mixtures processed by ERICA. The experimental results confirm the validity of the proposed method, which has been taken as the basis for the development of a low cost, non-invasive, termite detection system.

Keywords: Acoustic emission; Cumulant; ERICA; High order statistics (HOS); ICA; Termite detection; Vibratory signal

1. Introduction

Termites damage wood structures world-wide in an irreparable way. Most of this dramatic damage is caused by subterranean termites. The costs of this harm could be significantly reduced through earlier detection of the infestation. These methods

* Corresponding author. Tel.: +34 956028020; fax: +34 956028001.
E-mail address: juanjose.delarosa@uca.es (J.J. Gonzalez de la Rosa).

0263-2241/$ - see front matter © 2004 Elsevier Ltd. All rights reserved.
doi:10.1016/j.measurement.2004.08.002

of detection are also important because environmental laws are becoming more restrictive with termiticides due to their possible health threats.

The primary method of termite detection consists of looking for evidence of activity. But only about 25% of the building structure is accessible, and the conclusions depend on the level of expertise and the criteria of the inspector [1].

As a consequence, new techniques have been developed to remove subjectiveness and gain accessibility. But at best they are considered useful only as supplements. Acoustic methods have emerged as an alternative.

Termite activity takes place in wood, and when the wood fibers are broken they produce acoustic emissions. These acoustic signals are monitored using *ad hoc* resonant acoustic emission (AE) piezoelectric sensors which include microphones and accelerometers. User-friendly equipment is currently used in targeting subterranean insect infestations by means of spectral and temporal analysis. They have the drawback of the relative high cost and their practical limitations.

The usefulness of acoustic techniques for detection depends on several biophysical factors. The main one is the amount of distortion and attenuation as the sound travels through the soil ($\sim$600 dB m^{-1}, compared with 0.008 dB m^{-1} in the air). Furthermore, soil and wood are far from being ideal acoustic propagation media because of their high anisotropy and frequency dependent attenuation characteristics [2].

The aim of the present study is to investigate the capability of a robust ICA cumulant-based algorithm in the task of separating termite alarms signals which have been mixed with non-Gaussian random white noise. Termite alarms are considered as low-level transient signals. This is to show that a relatively economic microphone and a non-specific equipment can be used to collect data if the algorithm performs the task of separating.

AE data were recorded using a standard low-cost microphone and the sound card of a portable PC. A seismic accelerometer was previously used to characterize the frequency contents of the emissions. The experiment took place in the "Costa del Sol" (Malaga, Spain), and data taken from subterranean wood structures and roots.

Modern signal processing techniques can be used to distinguish insect sounds from background noise with good reliability in soil measurements, because sound insulating properties of soil help reduce interference. Besides, such techniques have been successfully used in relatively noisy urban environments.

These techniques are based mainly on spectral analysis and digital filtering. That is why they have been applied to data from acoustic *ad hoc* sensors and not to data recorded using standard microphones.

The particular contribution of this study is to show that an ICA-based method is capable of separating termite alarm signals, generated in wood and registered using a low cost sensor, from well-known signals. The alarm signals are low-noise patterns, recorded with a low-cost microphone and high-pass filtered. This could be the basis of separating low-level termite activity signals from background urban noise using a traditional PC and low cost non-invasive sensors.

The paper is structured as follows: Section 2 summarizes the methods for acoustic detection of termites; Section 3 defines the ICA model and outlines the characteristics of emissions in wood; Section 4 describes the experiments carried out. Conclusions are drawn in Section 5.

2. Acoustic detection of termites: characteristics and devices

2.1. Characteristics of the AE signals

Acoustic emission is defined as the elastic energy that is spontaneously released by materials undergoing deformation. This energy transfer through the material as a stress or strain wave and is typically detected using a piezoelectric transducer, which converts the surface displacement (vibrations) to an electrical signal.

Termites use a sophisticated system of vibratory long distance alarm. When disturbed in their nests and in their extended gallery systems, soldiers produce vibratory signals by drumming their heads against the substratum [3]. The drumming signals consist of trains of pulses which propagate

through the substrate (substrate vibrations), with pulse repetition rates (beats) in the range of 10–25 Hz, with burst rates around 500–1000 ms, depending on the species [4]. Soldiers produce such vibratory signals in response to disturbance (1–2 nm by drumming themselves) by drumming their head against the substratum. Workers can perceive these vibrations, become alert and tend to escape [5].

Fig. 1 shows a typical drumming signal produced by a soldier by taping its head against a chip of wood. It comprises two four-impulse bursts. Each of the pulses arises from a single, brief tap of the head against the wood.

AE data were acquired using the sound card of a portable PC and a low-cost standard microphone in low environmental noise conditions (in a basement), 1 m away from the site of the event. The signal amplitudes were highly variable and depend on the wood and strength of the taps. Thus, data are normalized to the maximum quantization level of the series.

Fig. 2 shows one of the impulses in a burst and its associated power spectrum is depicted in Fig. 3. Significant drumming responses are produced over the range 200 Hz–10 kHz. The carrier frequency of the drumming signal is around 2600 Hz.

The spectrum is not flat as a function of frequency as one would expect for a pulse-like event.

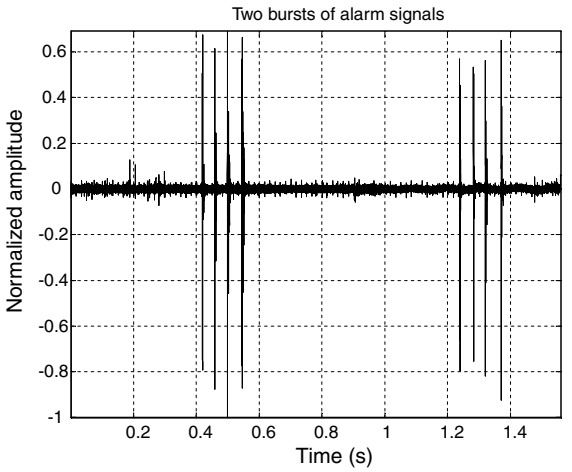

Fig. 1. Two bursts of a typical acoustic emission alarm signal produced by a soldier.

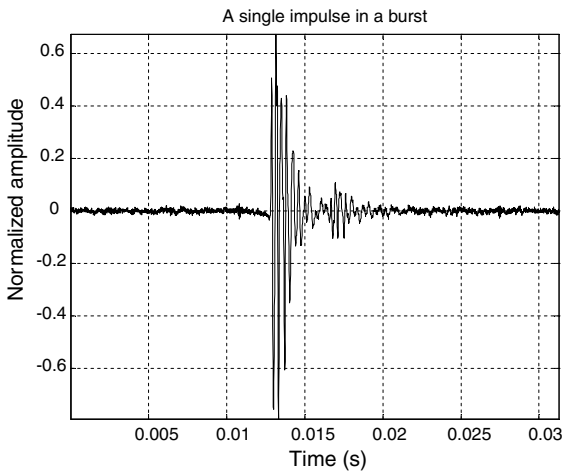

Fig. 2. A single pulse of a four-pulse burst.

This is due to the frequency response of the microphone (its selective characteristics) and also to the frequency-dependent attenuation coefficient of the wood.

Due to our identification purposes we are concerned of the spectral and time patterns of the signals; so we do not care about the energy levels. Besides during the demixing process of ICA original energy levels of the signals are lost.

2.2. Devices and ranges of measurement

Many efforts to develop techniques for detecting hidden termite infestations have produced only a few real alternatives to traditional visual inspection methods. Remarkable alternatives are ground-based monitoring devices and sensors that detect acoustic emissions of termites in wood. It has been proved that nearly all noise signals have most of their energy below 20 kHz [1] [3,5]. Besides, termite activities in the wood generate a significant amount of acoustic emission with frequency components extending to above 100 kHz. Therefore, acoustic emission sensors are successful because they are non-destructive and operate at high

[1] The sensor used was a model A3 resonant sensor (30–50 kHz) manufactured by Physical Acoustics, with a JFET low noise voltage amplifier, model 324-3.

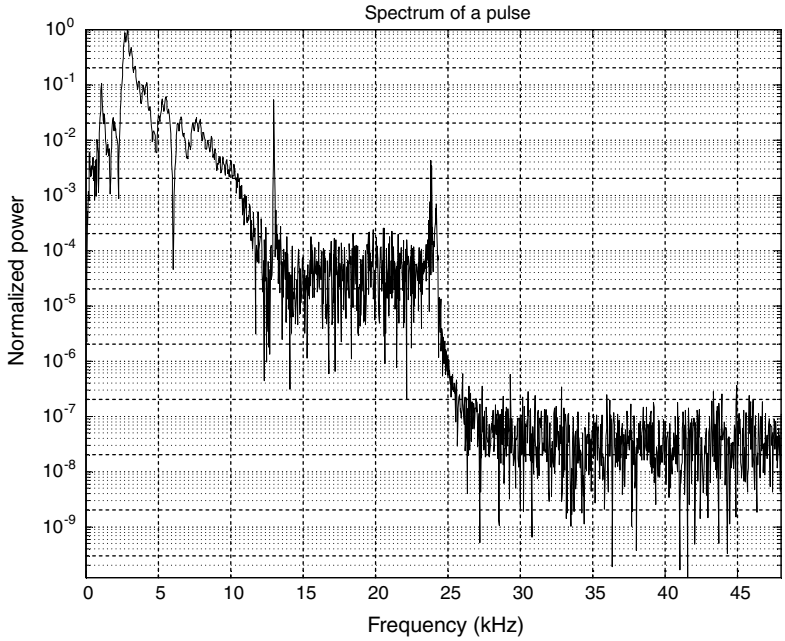

Fig. 3. Normalized power spectrum of a single pulse.

frequency (>40 kHz) where background noise is negligible and does not interfere with insect sounds [6]. Acoustic measurement devices have been used primarily for detection of termites (feeding and excavating) in wood, but there is also the need of detecting termites in trees and soil surrounding building perimeters. Soil and wood have a much longer coefficient of sound attenuation than air and the coefficient increases with frequency. This attenuation reduces the detection range of acoustic emission to 2–5 cm in soil and 2–3 m in wood, as long as the sensor is in the same piece of material [6]. The range of acoustic detection is much greater at frequencies <10 kHz, and low frequency accelerometers have been used to detect insect larvae over 1–2 m in grain and 10–30 cm in soil [1,6].

3. The ICA model

3.1. Outline of ICA

Blind source separation (BSS) by ICA is receiving attention because of its numerous applications in signal processing such as speech recognition, medicine and telecommunications [7]. The aim of ICA consists in the recovery of the unknown independent source signals that have been linearly mixed in the medium [8]. These mixtures (sensor observations) are the input data of the ICA algorithm [9]. In contrast to correlation-based algorithms such as principal component analysis (PCA), ICA not only applies second-order statistics (decorrelation of signals), but also reduces high-order dependencies with the goal of making the signals statistically independent [7,9]. The statistical methods in BSS are based in the probability distributions and the cumulants of the mixtures. The recovered signals (the source estimators) have to satisfy a condition which is modelled by a contrast function. This function is optimized and leads to an estimation of the mixing matrix and the original source signals. The underlying assumptions are the mutual independence among source signals and the non-singularity of the mixing matrix [7,9].

3.2. The ICA model and its properties

Let $\mathbf{s}(t) = [s_1(t), s_2(t), \ldots, s_m(t)]^{\mathrm{T}}$ be the vector of unknown source signals, where the superscript

represents transpose. Sources are statistically independent. If the probability density function (PDF) of an individual source entry is denoted as $p_i(s_i)$, independence implies the joint PDF can be expressed as the product of the marginal PDFs as

$$p(s) = \prod_{i=1}^{N} p_i(s_i) \tag{1}$$

Independence of the sources means one entry of a source signal provides no further information about any other [10]. The known mixture of the source signals is modelled by

$$\mathbf{x}(t) = \mathbf{A} \cdot \mathbf{s}(t) \tag{2}$$

where $\mathbf{x}(t) = [x_1(t), x_2(t), \ldots, x_m(t)]^{\mathrm{T}}$ is the available vector of observations and $\mathbf{A} = [a_{ij}] \in \Re^{m \times n}$ is the unknown mixing matrix, modelling the environment in which signals are mixed, transmitted and measured [11]. Without loss of generality we assume that $\mathbf{A}$ is a non-singular $n \times n$ square matrix. The goal of ICA is to find a non-singular $n \times m$ separating matrix $\mathbf{B}$ such that extract source signals via [12]

$$\hat{\mathbf{s}}(t) = \mathbf{y}(t) = \mathbf{B} \cdot \mathbf{x}(t) = \mathbf{B} \cdot \mathbf{A} \cdot \mathbf{s}(t) \tag{3}$$

where $\mathbf{y}(t) = [y_1(t), y_2(t), \ldots, y_m(t)]^{\mathrm{T}}$ is the separated source vector which is an estimator of the original vector of sources [13]. The separating matrix has a scaling freedom on each of its rows because the relative amplitudes of sources in $\mathbf{s}(t)$ and columns of $\mathbf{A}$ are unknown [12,7].

The process of ICA is depicted in the block diagram of Fig. 4.

The final transfer matrix $\mathbf{G} \equiv \mathbf{BA}$ relates the vector of independent original signals to its estimator. If the complete determination of the mixing matrix $\mathbf{A}$ were possible, $\mathbf{G}$ would be the identity. Another property of ICA relies on non-Gaussianity [14]. Gaussian distributed signals are inseparable because if individual sources had Gaussian distributions, the joint probability density function would look more than a Gaussian distribution than any entry [15]. When dealing with Gaussian signals, the joint distribution is invariant under linear transformations [16]. In order to formalize the principles of separation we introduce the following theorem.

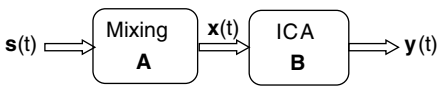

Fig. 4. Block diagram of the ICA model.

Theorem 1. (Darmois-Skitovich) *Let be the model described by Eq. (3) which verifies condition (1). Let be two components of the vector of estimated sources which are mutually independent*

$$\hat{s}_k = \sum_{i=1}^{n} g_{ki} s_i$$
$$\hat{s}_l = \sum_{j=1}^{n} g_{lj} s_j \tag{4}$$

If an index h exists which verifies that g_{kh} and g_{lh} are non-zero, then s_h is Gaussian.

As the outputs are mutually independent, $\mathbf{G}$ is an orthogonal matrix. This implies the following corollary.

Corollary 1. *Let be the model described by Eq. (3) which verifies condition 2. Let be a non-Gaussian component of the vector s. If the components of the vector y are mutually independent, then the separation is guaranteed.*

The mutual independence of the outputs only implies condition $\mathbf{GG}^{\mathrm{T}} = \mathbf{I}_n$. But if all the signals in vector s are non-Gaussian then $\mathbf{G} = \mathbf{I}_n$.

3.3. The implementation of the algorithm

3.3.1. Cumulants and moments

High order statistics, known as cumulants, are used to infer new properties about the data of a non-Gaussian process [17]. Before cumulants, due to the lack of analytical tools, such processes had to be treated as if they were Gaussian [18]. Cumulants, and their associated Fourier transforms, known as polyspectra, reveal information about amplitude and phase of the data, whereas second order statistic methods (power, variance, covariance and spectra) are phase-blind [20,18].

It is convenient to remark that cumulants of order higher than two are all zero in signals with Gaussian probability density functions. What is the same, cumulants are blind to any kind of a Gaussian process. This is the reason why it is not

possible to separate these signals using the statistical approach [19].

Let $\mathbf{x}(t) = [x_1(t), x_2(t), \ldots, x_r(t)]^{\mathrm{T}}$ be a vector of r zero-mean random variables. The rth moment of this vector of signals is [20]

$$\mu_r(\mathbf{s}) = E\{\mathbf{s}^r\} \tag{5}$$

where $\mathbf{E}$ is the mathematical expectation.

The relationship among the cumulant of r stochastic signals and their moments of order p, $p \leqslant r$, can be calculated by using the *Leonov-Shiryayev* formula [20]

$$\mathrm{Cum}(x_1, \ldots, x_r) = \sum (-1)^k \cdot (k-1)! \cdot E\left\{\prod_{i \in v_1} x_i\right\} \cdot E\left\{\prod_{j \in v_2} x_j\right\} \cdots E\left\{\prod_{k \in v_p} x_k\right\} \tag{6}$$

where the addition operator is extended over all the set of v_i $(1 \leqslant i \leqslant p \leqslant r)$ and v_i compose a partition of $1, \ldots, r$. For example, the set of indices of the components of $\mathbf{x}$, $I = \{1,2,3,4\}$. A partition of I is the unordered collection of non-intersecting non-empty sets I_p such that $\cup I_p = I$. The set of partitions corresponding to $r = 4$ is given in Table 1.

By using (6) the second-, third-, and fourth-order cumulants are given by:

$$\mathrm{Cum}(x_1, x_2) = E\{x_1 \cdot x_2\} \tag{7a}$$

$$\mathrm{Cum}(x_1, x_2, x_3) = E\{x_1 \cdot x_2 \cdot x_3\} \tag{7b}$$

$$\begin{aligned}\mathrm{Cum}(x_1, x_2, x_3, x_4) = {} & E\{x_1 \cdot x_2 \cdot x_3 \cdot x_4\} \\ & - E\{x_1 \cdot x_2\}E\{x_3 \cdot x_4\} \\ & - E\{x_1 \cdot x_3\}E\{x_2 \cdot x_4\} \\ & - E\{x_1 \cdot x_4\}E\{x_2 \cdot x_3\}\end{aligned} \tag{7c}$$

Table 1
Partitions corresponding to $r = 4$

Order	Set of partitions
1	{(1, 2, 3, 4)}
2	{(1), (2, 3, 4)}, {(2), (1, 3, 4)}, {(3), (1, 2, 4)}, {(4), (1, 2, 3)}, {(1, 2), (3, 4)}, {(1, 3), (2, 4)}, {(1, 4), (2, 3)}
3	{(1), (2), (3, 4)}, {(1), (3), (2, 4)}, {(2), (3), (1, 4)}, {(1), (4), (2, 3)}, {(2), (4), (1, 3)}, {(3), (4), (1, 2)}
4	{(1), (2), (3), (4)}

In the case of nonzero mean variables x_i have to be replaced by $x_i - E\{x_i\}$. Let $\{x(t)\}$ be a rth-order stationary random process. The rth-order cumulant is defined as the joint rth-order cumulant of the random variables $x(t)$, $x(t+\tau_1), \ldots, x(t+\tau_{r-1})$,

$$\begin{aligned}&C_{r,x}(\tau_1, \tau_2, \ldots, \tau_{r-1}) \\ &\quad = Cum[x(t), x(t+\tau_1), \ldots, x(t+\tau_{r-1})]\end{aligned} \tag{8}$$

For stationary random processes the rth-order cumulant is only a function of $r-1$ lags. If $\{x(t)\}$ is nonstationary then the rth-order cumulant includes time dependency. For a zero-mean stationary process and for $r = 3,4$, the rth-order cumulant can also be defined as

$$\begin{aligned}\mathrm{Cum}(\tau_1, \tau_2, \ldots, \tau_{r-1}) = {} & E\{x(\tau_1) \cdots x(\tau_{r-1})\} \\ & - E\{g(\tau_1) \cdots g(\tau_{r-1})\}\end{aligned} \tag{9}$$

where $\{g(t)\}$ is a Gaussian random process with the same second order statistics as $\{x(t)\}$. Therefore, cumulants also conveys a measure of the distance of a random process from Gaussianity [20].

The second-, third- and fourth-order cumulants of zero-mean $x(t)$ can be expressed using (7) and (8).

$$C_{2,x}(\tau) = E\{x(t) \cdot x(t+\tau)\} \tag{10a}$$

$$C_{3,x}(\tau_1, \tau_2) = E\{x(t) \cdot x(t+\tau_1) \cdot x(t+\tau_2)\} \tag{10b}$$

$$\begin{aligned}&C_{4,x}(\tau_1, \tau_2, \tau_3) \\ &\quad = E\{x(t) \cdot x(t+\tau_1) \cdot x(t+\tau_2) \cdot x(t+\tau_3)\} \\ &\quad = C_{2,x}(\tau_1) - C_{2,x}(\tau_2 - \tau_3) \\ &\quad = C_{2,x}(\tau_2) - C_{2,x}(\tau_3 - \tau_1) \\ &\quad = C_{2,x}(\tau_3) - C_{2,x}(\tau_1 - \tau_2)\end{aligned} \tag{10c}$$

By putting $\tau_1 = \tau_2 = \tau_3 = 0$ in (10), we obtain

$$\gamma_{2,x} = E\{x^2(t)\} = C_{2,x}(0) \tag{11a}$$

$$\gamma_{3,x} = E\{x^3(t)\} = C_{3,x}(0,0) \tag{11b}$$

$$\gamma_{4,x} = E\{x^4(t)\} - 3(\gamma_{2,x})^2 = C_{4,x}(0,0,0) \tag{11c}$$

Eqs. (11) are the measures of the variance, skewness and kurtosis of the distribution in terms of cumulants at zero lags. Normalized kurtosis and skewness are defined as $\gamma_{4,x}/(\gamma_{2,x})^2$ and $\gamma_{3,x}/(\gamma_{2,x})^{3/2}$,

respectively. We will use and refer to normalized quantities because they are shift and scale invariant. If $x(t)$ is symmetric distributed, its skewness is necessarily zero (but not vice versa); if $x(t)$ is Gaussian distributed, its kurtosis is necessarily zero (but not vice versa).

3.3.2. Contrast functions

It has been proved that a set of random variables are statistically independent if their cross-cumulants are zero [12].

Cumulants can be used to define contrast functions. The contrast function, $\Phi[y]$, verifies

$$\Phi[y] = \Phi[BAs] \geqslant \Phi[s] \tag{12}$$

in order to be minimized. A criteria chosen to obtain the contrast function is to minimize the distance between the cumulants of the sources $\mathbf{s}(t)$ and the outputs $\mathbf{y}(t)$.

In a real situation sources are unknown so it is necessary to use contrast functions which involve only the observed signals. In our case we use an entropic function in the terms described in the following [21].

Theorem 2. *Separation of the sources can be developed using the following contrast function based on the entropy of the outputs*

$$H(\boldsymbol{z}) = H(\boldsymbol{s}) + \log[\det(\boldsymbol{G})] - \sum \frac{\boldsymbol{C}_{1+\beta,y_i}}{1+\beta} \tag{13}$$

where $\boldsymbol{C}_{1+\beta,y_i}$ is the $1+\beta$th-order cumulant of the ith output, z is a non-linear function of the outputs y_i, s is the source vector, G is the global transfer matrix of the ICA model and $\beta > 1$ is an integer verifying that $\beta + 1$ order cumulants are non-zero.

Using the above contrast function it can be shown [21] that the separating matrix can be obtained by means of the following recurrent equation

$$\mathbf{B}^{(h+1)} = \left[\mathbf{I} + \mu^{(h)}\left(\mathbf{C}_{y,y}^{1,\beta}\mathbf{S}_y^{\beta} - I\right)\right]\mathbf{B}^{(h)} \tag{14}$$

where $\mathbf{S}_y^{\beta}$ is the matrix of the signs of the output cumulants. Eq. (14) can be interpreted as a quasi-Newton algorithm of the cumulant matrix $\mathbf{C}_{y,y}^{1,\beta}$. The learning rate parameters $\mu^{(h)}$ and η are related by

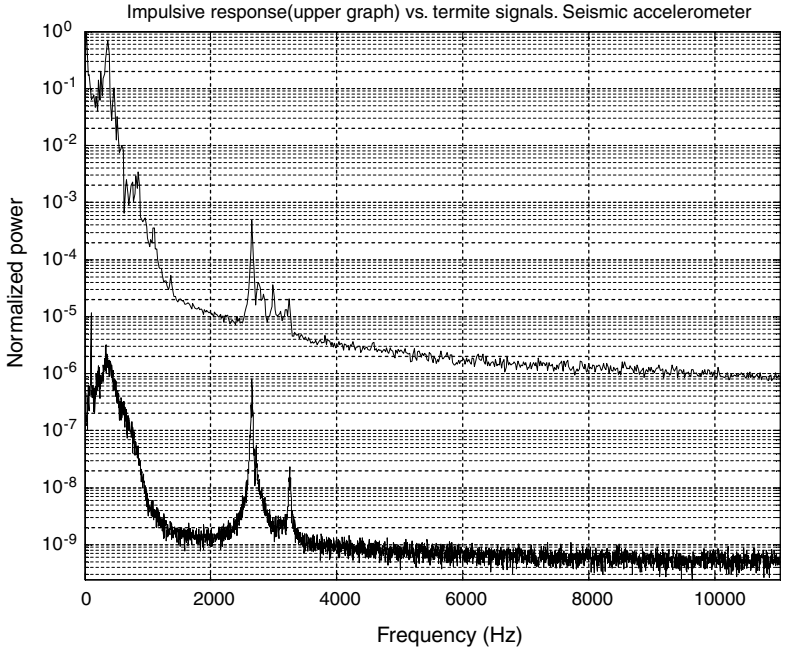

Fig. 5. Comparison between impulsive response and spectrum of vibratory alarm signals.

$$\mu^{(h)} = \min\left(\frac{2\eta}{1+\eta\beta}, \frac{\eta}{1+\eta\left\|\mathbf{C}_{y,y}^{1,\beta}\right\|_p}\right) \quad (15)$$

with $\eta < 1$ to avoid $\mathbf{B}^{(h+1)}$ being singular; $\|.\|_p$ denotes the p-norm of a matrix.

The adaptative Eq. (14) converges, if the matrix $\mathbf{C}_{y,y}^{1,\beta}\mathbf{S}_y^{\beta}$ tends to the identity.

The following sections describe the results we obtained by the application of the method described above.

4. Results and discussions

The experiment carried out comprises two stages. The first one handles the original signals once they have been high-pass filtered. In the second part of the experiment we consider the signals without pre-processing. This division was thought to perform a preliminary experiment which handles trains of pulses as sources, without any coupling from the media.

Vibratory signals were collected in a basement of a building located in the *Costa del Sol* (southern Spain). Due to the quiet conditions it was easy to ear termites drumming, and we used an economical directional microphone, *Ariston* CME6 model, with a sensibility of 62 ± 3 (dB) and a bandwidth of 100 Hz–8 kHz. The device was connected to the sound card of a portable computer and the sample frequency was adjusted to 96,000 Hz.

These ideal conditions were thought to in order to collect non-contaminated data. In the first stage time series were high-pass filtered in the lab to sup-

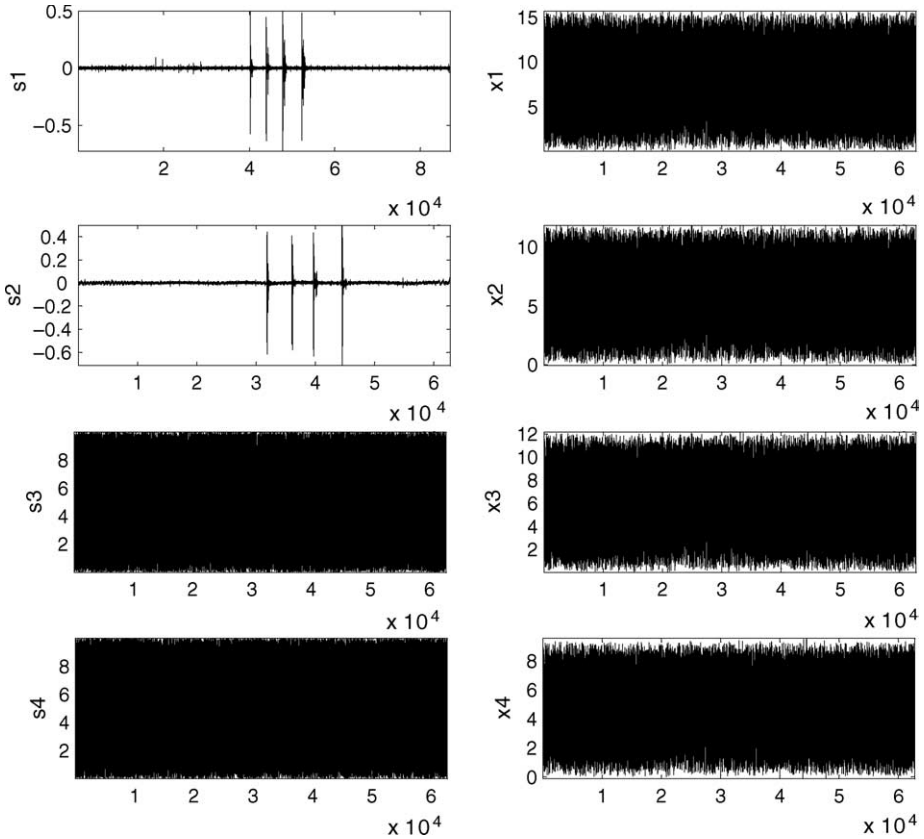

Fig. 6. The filtered and simulated source signals and their mixtures. Horizontal units: 1/96,000 (s).

press low-frequency coupling signals introduced by the microphone and the environment which are non-relevant in the first set of signals. We obtained two zero-mean normalized bursts (like ones of Fig. 1) as sources 1 and 2. The computed normalized kurtosis are 212.93, and 211.09, respectively; which shows that ICA is expected to work with the measured acoustic data.

In both parts of the experiment we used four sources as the inputs of the model. The third and forth sources consist of two uniform distributed noise signals with enough amplitude to mask the burst once the mixture was done. The mixing matrix is a 4×4 random matrix whose elements are chosen from uniformly distributed random numbers within 0 and 1. No pre-whitened was applied in order to manipulate four mixtures. Furthermore, we have proved that whitening suppresses three of the mixtures.

In order to compare this method with traditional methods based on power spectrum comparisons, we obtain the power spectrum of the separated signals and compare it with the power spectrum of vibratory signals (original sources) First of all we have to characterize the spectrum corresponding to this specie of termite (*reticulitermes grassei*).

4.1. Power spectra characteristics

In order to obtain a reference to compare with *ad hoc* references were consulted. AE detection methods based on energy conservation principles work under the hypothesis of considering the vibratory signals as pulse trains. So we have to compare a lab-impulse frequency response of the sensor to the real frequency response when the sensor is excited with the vibratory signals. We have

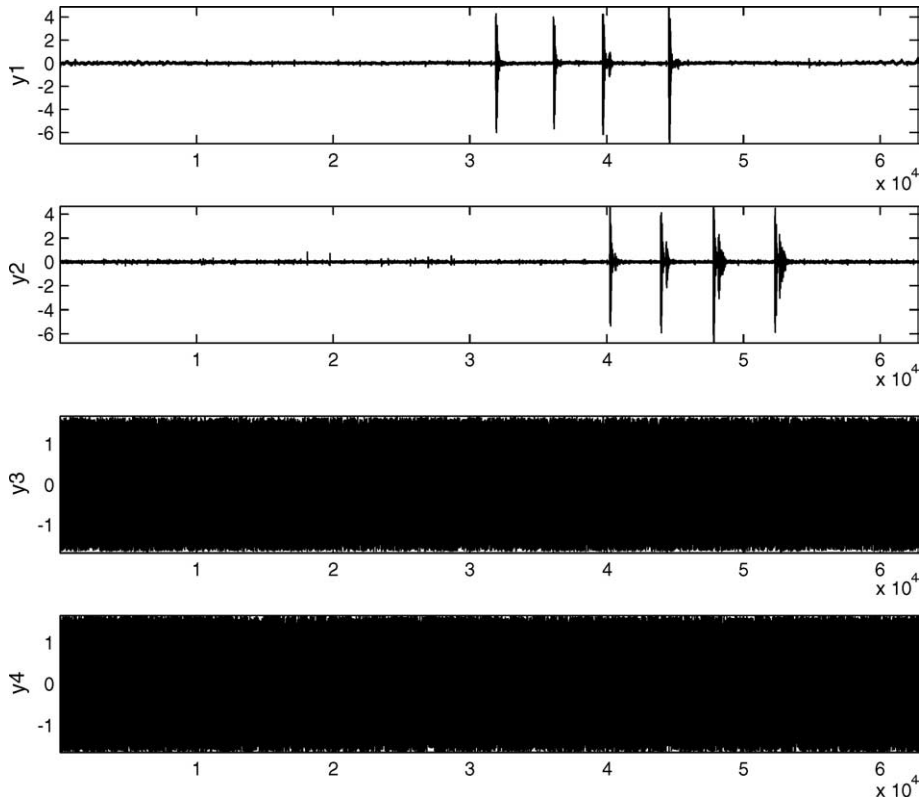

Fig. 7. The separation results by the ICA algorithm. Horizontal units: 1/96,000 (s).

to see if carrier frequencies match. If it is the case, the detection has been carried out and the pattern of the spectrum is the reference which indicates a vibratory signal is present.

This characterization process was developed with data from a seismic accelerometer (KB12V, MMF). Fig. 5 shows a comparison between the impulse response (upper graph) of the accelerometer and the spectrum of the data series corresponding to drumming signals. The traditional procedure used to detect termite alarms consists of comparing the frequencies of the maxima of these two spectra. The comparison let us conclude the same 2600 Hz peak corresponding to the carrier frequency. So, this is the reference frequency.

These criteria were considered in the first stage of the experiment in order to check if carrier frequency is present in the spectra of the outputs. The first stage is presented first.

4.2. Filtered pulse trains as original sources

Fig. 6 shows the original filtered sources and the mixed results. Mixed signals give very little information about the original sources. The ERICA separated results are shown in Fig. 7.

Comparing the separated results with the source signals in Fig. 6, a number of differences are found. First, the amplitudes are amplified to some extent due to the changes in the demixing matrix, implying that original amplitude (energy) information has lost. Second, there are time shifts between the original sources and the recovered signals. Third, the sequences are arranged as the same way as the original.

Figs. 8 and 9 show the qualitative evaluation of the performance of the algorithm. Fig. 7 show wide area geometric patterns, which let us conclude that mixtures are composed by random numbers.

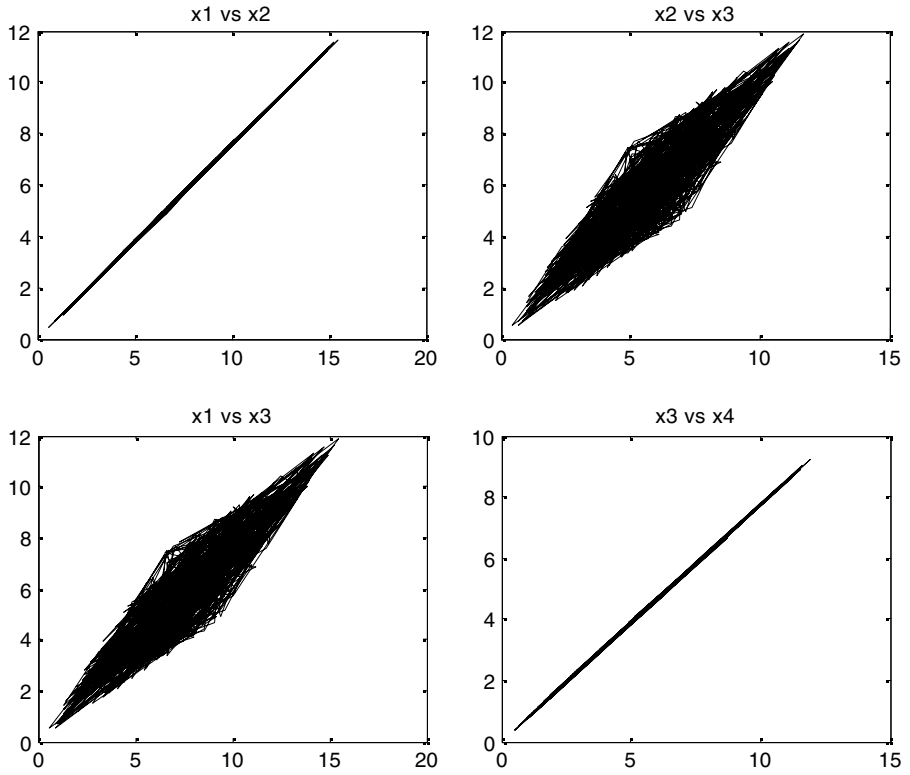

Fig. 8. The lag–lag representation of the mixtures.

On the other hand, Fig. 8 comprises more informative graphs. The comparison between s_1 vs. s_2 and y_1 vs. y_2 graph yields a very similar pattern which leads us to very similar signals. The rest

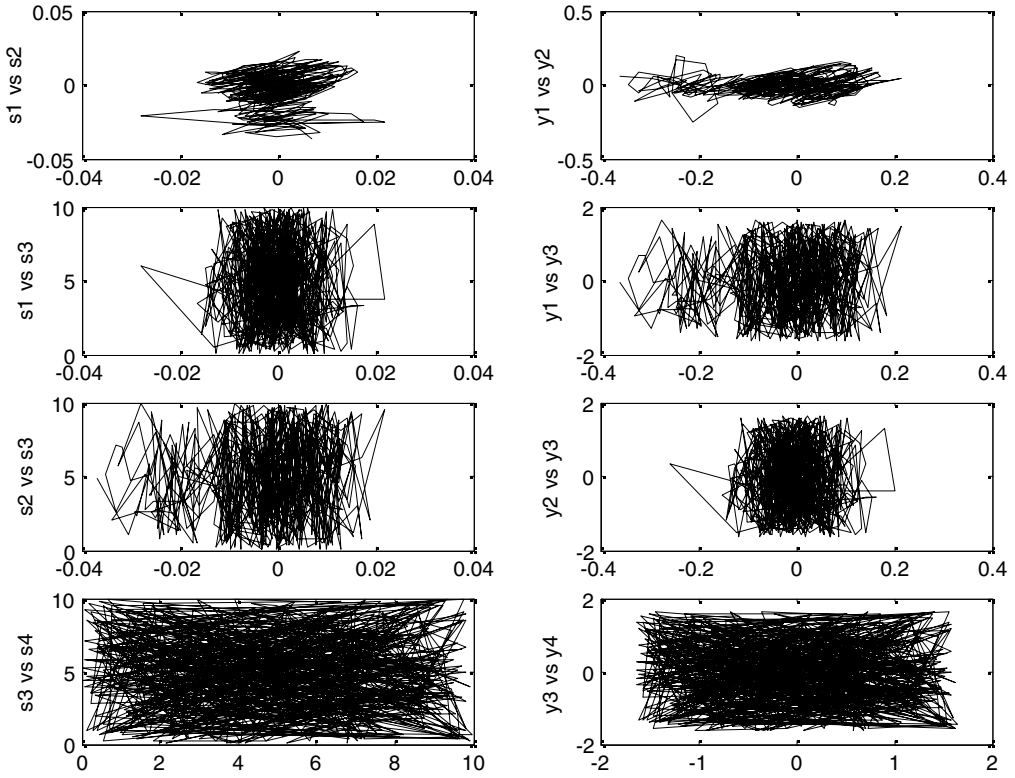

Fig. 9. The lag–lag representation of the estimated (separated) signals.

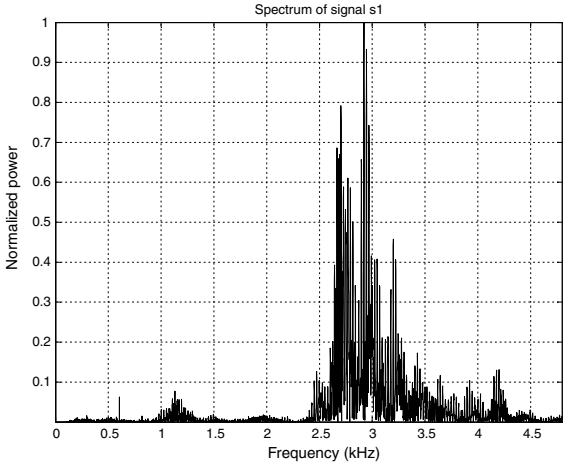

Fig. 10. Normalized power spectrum of source 1.

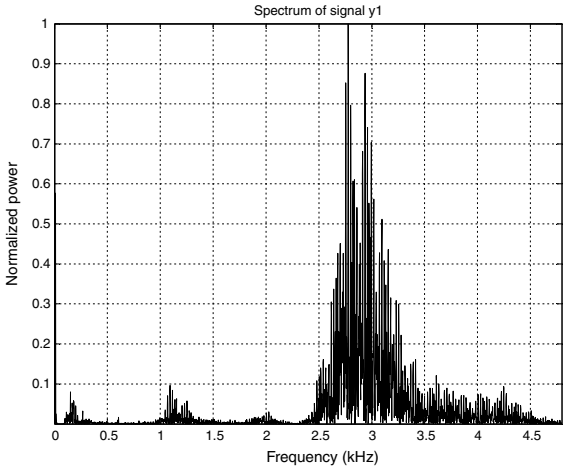

Fig. 11. Normalized power spectrum of output 1.

of the graphs are not as explicit, but it can be observed similarities between source patterns and measured patterns.

Figs. 10–12 show the normalized power spectra corresponding to one source and the two impulsive outputs, respectively.

The spectra of the separated signals $y_1(t)$ and $y_2(t)$ show the same carrier frequency. So we can confirm the validity of the ERICA method based on the traditional spectra-based method.

4.3. Non-Filtered pulse trains as original sources

Signals without pre-processing are considered here. Fig. 13 shows the original sources and the mixtures. No lag–lag graphs are depicted because they exhibit a similar shape to those in Fig. 9.

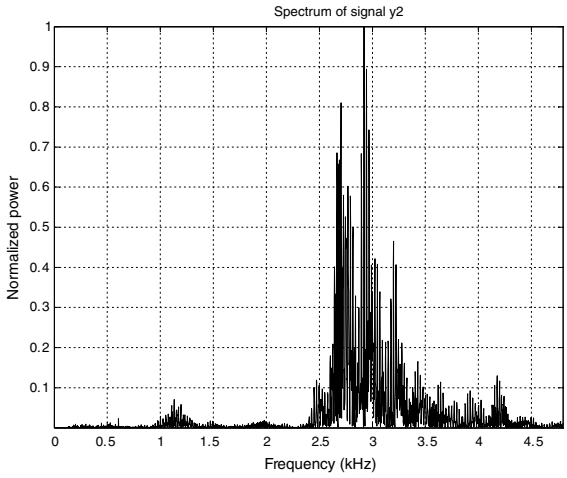

Fig. 12. Normalized power spectrum of output 2.

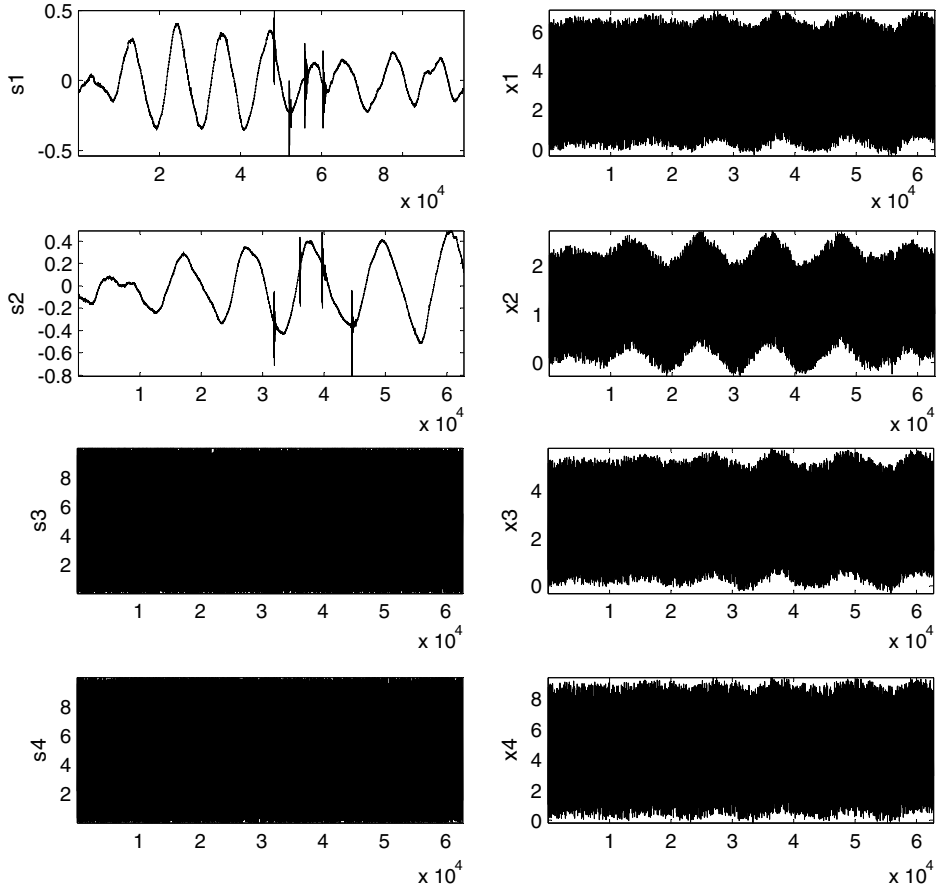

Fig. 13. The real and simulated source signals and their mixtures. Horizontal units: 1/96,000 (s).

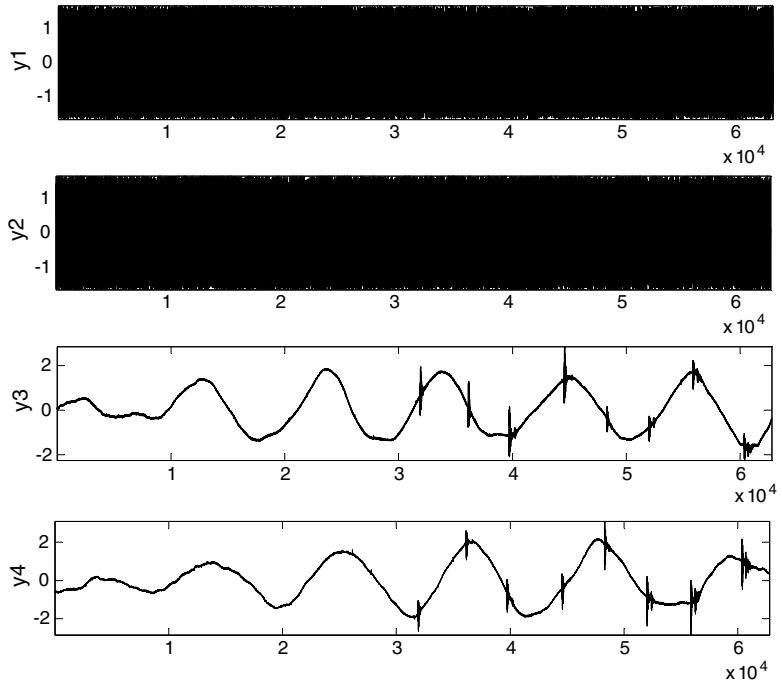

Fig. 14. The separation results by the ICA algorithm. Horizontal units: 1/96,000 (s).

The outputs of the algorithm are depicted in Fig. 14. It is seen that the algorithm considers the two bursts as if they had the same origin.

It is not necessary to perform a frequency-domain comparison because it was developed with filtered signals. Besides, the spectra exhibit maxima point in the low-frequency interval near DC.

5. Conclusion

The independent component analysis has been presented in this paper as a novel method used to detect vibratory signals from termite activity in wood. This ICA method is far different from traditional energy conservation-based methods, as power spectrum, which obtain an energy diagram of the different frequency components, with the risk that low-level sound can be masked.

This experience demonstrates that the algorithm ERICA is able to separate the sources with whatever small energy levels. This is due to the fact that ICA is based on the statistical independence of the components and not in the energy associated to each frequency component. This conclusion can be expanded.

From the results of the spectra in the first stage of the experience it is clear that the separation task has been performed correctly. This is so because the same spectral shape is outlined. In this stage we have proved the validity of ICA over a preprocessed set of signals.

The second stage confirms the performance of the algorithm ERICA in the sense that it joins the two bursts in one. This means that only an insect (one emitter) should be considered. This is the situation we had in practice.

Besides, ICA can be a useful tool to identify sounds produced by insects and to study them in detail.

From the device point of view, it has been proved that a low-cost microphone can be used for insect-detection purposes. This is so because in case of high-level background noise, even if it is white, as it has been proved, ICA is capable of extracting the burst of impulses. This means that

accelerometers-based equipment could be displaced when it is not needed a high sensitive device. In the case of a high sensibility requirement, accelerometers can be used to extract distorted information which would be ICA processed to extract the possible vibratory signals produced by insects.

Finally, we attend the bandwidth specification of the AE sensor. Traditional methods compare the impulsive response of the AE sensor with the spectrum of the acquired signal, based on the hypothesis that bursts produced by termites comprise straight pulses [1]. In the case of an ICA method of detection, no frequency-domain comparison is needed; a time-domain characterization is enough.

Further experiments will be developed in residential zones where background noise is high and where coloured noise is present. This would be the next step in checking the performance.

References

[1] W. Robbins, R. Mueller, T. Schaal, T. Ebeling, Characteristics of acoustic emission signals generated by termite activity in wood, in: Proceedings of the IEEE Ultrasonic Symposium, 1991, pp. 1047–1051.

[2] R. Mankin, J. Fisher, Current and potential uses of acoustic systems for detection of soil insects infestations, in: Proceedings of the Fourth Symposium on Agroacoustic, 2002, pp. 152–158.

[3] A. Röhrig, W. Kirchner, R. Leuthold, Vibrational alarm communication in the African fungus-growing termite genus macrotermes (isoptera, termitidae), Insectes Sociaux 46 (1999) 71–77.

[4] S. Connétable, A. Robert, F. Bouffault, C. Bordereau, Vibratory alarm signals in two sympatric higher termite species: Pseudacantotermes spiniger and p. militaris (termitidae, macrotermitinae), Journal of Insect Behavior 12 (3) (1999) 90–101.

[5] J. Reinhard, J.-L. Clément, Reaction of European reticulitermes termites to soldier head capsule volatiles (isoptera, rhinotermitidae), Journal of Insect Behavior 15 (1) (2002) 95–107.

[6] R. Mankin, W. Osbrink, F. Oi, J. Anderson, Acoustic detection of termite infestations in urban trees, Journal of Economic Entomology 95 (5) (2002) 981–988.

[7] A. Hyvärinen, E. Oja, Independent Components Analysis: A Tutorial, Laboratory of Computer and Information Science, Helsinki University of Technology, 1999.

[8] C. Puntonet, New algorithms of source separation in linear media, Ph.D. thesis, Department of Architecture and Technology of Computers, University of Granada, Spain, 1994.

[9] S. Cruces, L. Castedo, A. Cichocki, Robust blind source separation algorithms using cumulants, Neurocomputing 49 (2002) 87–118.

[10] T. Lee, M. Girolami, A. Bell, A unifying information-theoretic framework for independent component analysis, Computers and Mathematics with Applications 39 (2000) 1–21.

[11] J. Zhu, X.-R. Cao, Z. Ding, An algebraic principle for blind source separation of white non-Gaussian sources, Signal Processing 79 (1999) 105–115.

[12] B. Prieto, New algorithms of blind source separation using geometric methods, Ph.D. thesis, Department of Architecture and Technology of Computers, University of Granada, Spain, 1999.

[13] J. Cardoso, Blind signal separation: statistical principles, Proceedings of the IEEE 9 (10) (1988) 2009–2025.

[14] A. Mansour, A. Barros, N. Onishi, Comparison among three estimators for higher-order statistics, in: The Fifth International Conference on Neural Information Processing, Kitakyushu, Japan, 1998.

[15] W. Li, F. Gu, A. Ball, A. Leung, C. Phipps, A study of the noise from diesel engines using the independent component analysis, Mechanical Systems and Signal Processing 15 (6) (2001) 1165–1184.

[16] F. Ham, N. Faour, Infrasound signal separation using independent component analysis, Sponsored by the Boeing Company, 2002, Contract No. 7M210007.

[17] M. Hinich, Detecting a transient signal by bispectral analysis, IEEE Transactions on Acoustics 38 (9) (1990) 1277–1283.

[18] A. Swami, J. Mendel, C. Nikias, Higher-Order Spectral Analysis Toolbox User's Guide, 2001.

[19] C. Nykias, J. Mendel, Signal processing with higher-order spectra, IEEE Signal Processing Magazine (1993) 10–37.

[20] J. Mendel, Tutorial on higher-order statistics (spectra) in signal processing and system theory: theoretical results and some applications, Proceedings of the IEEE 79 (3) (1991) 278–305.

[21] S. Cruces, A unified view of blind source separation algorithms, Ph.D. thesis, Signal Processing Department, University of Vigo, Spain, 1999.